# COMPUTER ARCHITECTURE WITH ASSOCIATIVE PROCESSOR REPLACING LAST LEVEL CACHE AND SIMD ACCELERATOR

L. Yavits, A. Morad, R. Ginosar

**Abstract**—This study presents a novel computer architecture where a last level cache and a SIMD accelerator are replaced by an Associative Processor. Associative Processor combines data storage and data processing and provides parallel computational capabilities and data memory at the same time. An analytic performance model of the new computer architecture is introduced. Comparative analysis supported by simulation shows that this novel architecture may outperform a conventional architecture comprising a SIMD coprocessor and a shared last level cache while consuming less power.

**Index Terms**— Multicore, SIMD, Associative Processor, Analytical Performance Models.

## 1 Introduction and Related Work

Many of today's computing architectures include vector, or SIMD coprocessors [1], [2], [3]. The efficiency of SIMD processors is limited by memory bandwidth, or by number of computations performed per memory transaction [4]. Data transfer between processing elements (PEs) and memory hierarchies curbs the full utilization of SIMD parallel processing capabilities. High utilization of SIMD coprocessor requires very high computation-to-bandwidth ratio and large data sets [5].

Under such optimal operating conditions (when most of the time is spent on computation rather than on data transfer), arrays of computing elements in SIMD processors are very active, resulting in high power density and hotspots, creating additional design constraints such as power delivery, heat dissipation and high leakage power [6].

Power dissipation and on-chip communication are among the main factors limiting the scalability of multicore and manycore architectures [7]. Data transfers among storage and processing elements, among individual memories of a parallel processor, or among different memory hierarchies, lead to wasting energy on non-processing tasks and limit the speedup of multicore architectures [8].

The *associative processor* is a viable alternative to conventional SIMD systems [9], [10]. Traditional associative processors can perform any arithmetic operation on massive amounts of data in parallel. They essentially comprise a modified Content Addressable Memory, enabling processing in addition to content addressable access. They also allow normal access to the memory, similar to any RAM array. As such, the associative processor provides both massively parallel computational capabilities and data storage at the same time, offering performance speedup when executing parallel workloads, and making a dedicated SIMD accelerator redundant.

In this study we propose replacing the last level cache (LLC) of the baseline CPU architecture (Fig. 1(a)), or the combination of the LLC and a dedicated SIMD coprocessor (Fig. 1(b)), by an associative processor (Fig. 1(c)). The goals we set to achieve are as follows:

- Convert the data cache into a massively parallel processor capable of performing a variety of parallel compute-bound tasks.
- Eliminate a power- and bandwidth-limited dedicated SIMD coprocessor.
- Combine data storage and data processing and eliminate performance degradation and energy dissipation due to massive data transfers.

The associative processor is to be operated in two modes:

- *Conventional Cache mode*, in which the associative processor is operated as data RAM during the execution of the sequential portion of a program;
- *Associative Processing mode*, in which the parallelizable portion of a program is executed on the associative processor, where the data is stored.

The associative processor delivers a number of advantages over a conventional SIMD architecture:

- Data processing and data storage are unified. When the parallelizable portion of the program is due for execution, no data needs to be transferred from the shared memory to the processing units and back;
- Two basic operations of associative processor are essentially standard memory operations: write and read. The third basic operation, *compare,* is implemented similarly to read, and is performed along memory rows rather than columns. Therefore the per-bit power consumption of the associative processor is almost identical to that of RAM, which may have order of magnitude lower active power (and

- *Leonid Yavits (*), E-mail: yavits@tx.technion.ac.il.*
- *Amir Morad (*), E-mail: amirm@tx.technion.ac.il.*
- *Ran Ginosar (*), E-mail: ran@ee.technion.ac.il.*

*(*) Authors are with the Department of Electrical Engineering, Technion-Israel Institute of Technology, Haifa 32000, Israel.*

lower leakage power) per area than logic [11];

- In conventional cache mode, use of CAM instead of RAM enables full associativity. Consequently, it may allow reduction of hardware and software complexity of the cache (for example, the elimination of costly tag array circuitry), as well as elimination of conflict (interference) misses.
- There are fewer hotspots. Power is distributed uniformly over the entire processing array rather than being concentrated around processing units as in the case of conventional SIMD. Since leakage power may exponentially depend on temperature [6], this could be a significant advantage.

The drawback in replacing the LLC by the associative processor is that the effective cache size in the conventional cache mode is nearly halved, since the associative processor bit cell is about twice the size of a RAM cell (Fig. 3). This leads to certain performance degradation during the execution of the sequential portion of a workload, but the speedup achieved during the execution of the parallel portion of the workload yields a significant improvement in the overall system performance.

The rest of this paper is organized as follows. Section 2 provides a detailed description of an associative processor. Section 3 presents analytical modeling of associative processor and compares it, analytically and through simulation, to a conventional SIMD processor. Section 4 provides comparative performance and power consumption analysis of the three architectures of Fig. 1. Section 5 offers conclusions.

## 2 THE ASSOCIATIVE PROCESSOR

The associative processor is basically a Content Addressable Memory (CAM) with an ability to simultaneously write into multiple memory rows, making it an Associative Processor (AP) array rather than CAM array. A subset of the rows can be tagged during an associative search, and certain fields of these tagged rows can subsequently be updated in parallel.

The associative processor is depicted in Fig. 2. AP array is surrounded by several special registers: The mask register defines the active fields for write and read operations. The tag register tags the rows that are matched by the compare operation for the following write operation. The associative processor requires a controller, or sequencer, and an instruction cache (the CPU may serve as the controller). An optional Interconnect allows processing elements of the associative processor to communicate in parallel. Since associative processing operation is mainly bit-serial and processing elements do not store large amounts of temporary data, the Interconnect can be a relatively simple circuit switched network. Depending on workload, inter-PE communication requirements vary from no communication at all (for "embarrassingly parallel" tasks such Black-Scholes option pricing) to relatively intense communications (e.g., for dense matrix multiplication). Sometimes, support for special pre-defined communication patterns or permutations can be of advantage (e.g., for FFT). A possible implementation of a static-memory associative processor cell is shown in Fig. 3.

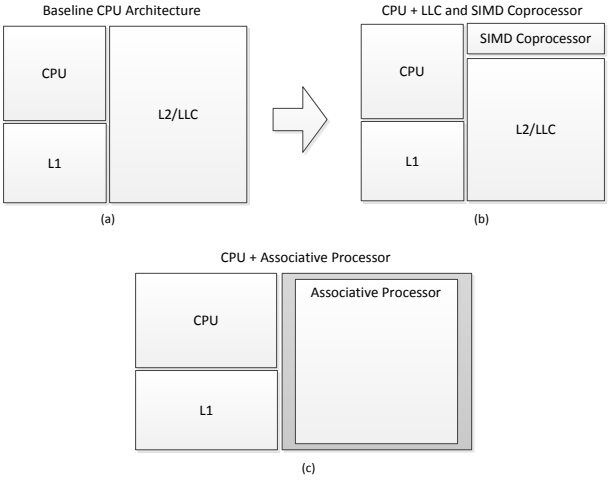


Fig. 1. (a) Baseline CPU with the LLC, (b) CPU with the LLC and the SIMD coprocessor, (c) CPU with the associative processor replacing the LLC.

The central part of the cell is identical to a conventional SRAM cell. In order to write data to memory through the top port, the Bit and Bit' lines are set and the Word line is asserted. To read data from memory (conventionally, through the top port), the Bit and Bit' lines are precharged and the Word line is asserted. Write and read operations are enabled only in the columns whose mask bits are set. To compare the data stored in memory (the entire row, a field or a single bit cell), the Match line is precharged and the inverted comparand (the value to compare with) is set on Bit and Bit' lines (for the columns that take no part in comparison, both Bit and Bit' lines are set to 0). If all bits in the fields to be compared match the comparand, the Match line remains high and a "1" is written into the side tag register (Fig. 2). If at least one bit is not matched, the Match line discharges and "0" is written into the tag bit.

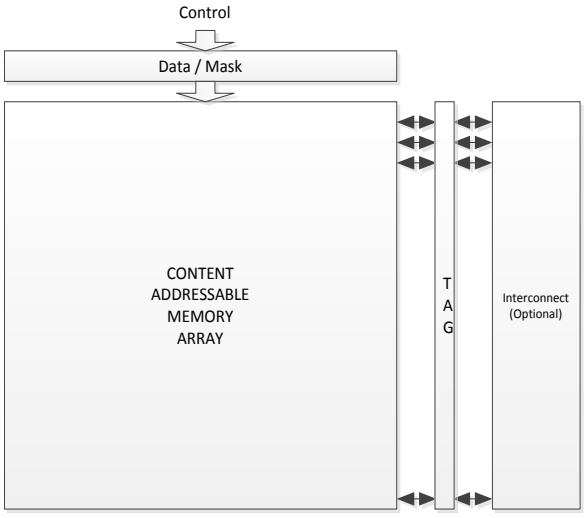


Fig. 2. Associative Processor – Conceptual View

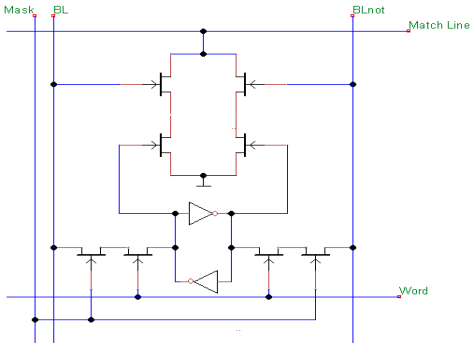

Fig. 3. NOR-type Associative Processor Cell

A number of AP cells that share Word and Match lines comprise a processing element. Typically one AP row corresponds to one associative processing element, but in general a processing element can occupy part of the AP row through a number of adjacent AP rows. The size of the associative processing element is limited by the Match and Word line delays.

Arithmetic operations in the associative processor can be performed in parallel on all processing elements, but are usually done in word-parallel, bit-serial manner. A possible implementation of vector addition is as follows [12]: The $m$ bit vectors A and B are added and the result is written over B; C is the carry bit. In Fig. 4, the $k^{th}$ vector elements $A_k$, $B_k$ and $C_k$ are stored and processed by the $PE_k$. The $m$ bit addition is carried out in $m$ bit-addition steps: $c_{i+1}|s_i = a_i + b_i + c_i$, where $i = 0, \dots, m-1$. One-bit addition (TABLE 1) is carried out in a series of passes, where in each pass, one entry of the truth table (a three bit input pattern – see TABLE 1) is matched against the contents of the entire AP array and the matching rows (processing elements) are tagged; then the logic result (two-bit output of the truth table in TABLE 1) is written into all tagged rows. During this operation, all but three input bit columns and two output bit columns of the associative array are masked out in each pass. Some input combinations do not change the output and therefore can be skipped. Since the operation overwrites one of the inputs, computation must be carried out according to the order indicated in the comments in TABLE 1.

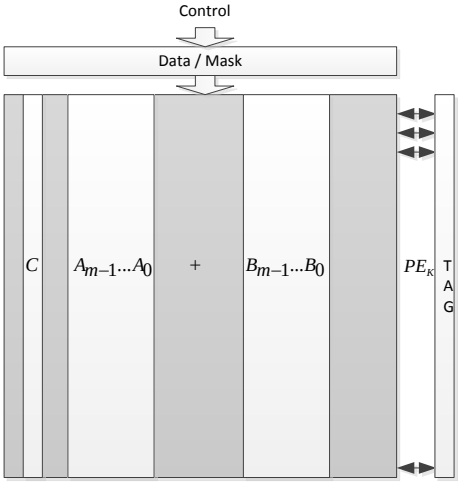

Fig. 4. Addition Example

TABLE 1
IMPLEMENTING FULL ADDER IN AP

| Entry | Input C | Input B | Input A | Output C | Output B | Comments |
|---|---|---|---|---|---|---|
| 0 | 0 | 0 | 0 | 0 | 0 | No action |
| 1 | 0 | 0 | 1 | 0 | 1 | 2nd pass |
| 2 | 0 | 1 | 0 | 0 | 1 | No action |
| 3 | 0 | 1 | 1 | 1 | 0 | 1st pass |
| 4 | 1 | 0 | 0 | 0 | 1 | 3rd pass |
| 5 | 1 | 0 | 1 | 1 | 0 | No action |
| 6 | 1 | 1 | 0 | 1 | 0 | 4th pass |
| 7 | 1 | 1 | 1 | 1 | 1 | No action |

*Pass = COMPARE cycle followed by WRITE cycle*

As can be seen from TABLE 1, four compare and write operations are required to complete one-bit addition. Therefore, fixed point $m$ bit addition takes $O(m) = 8m$ cycles. Subtraction and comparison operations are performed similarly and require a similar number of cycles.

Fixed precision multiplication and division in associative processor are implemented by long multiplication and long division respectively, consisting of a series of add-shift and subtract-shift operations, executed bit-serially. The addition or subtraction are done as described above (multiplication is usually done "MSB first"), while shift is implemented by activating different bit columns and therefore requires no cycles. The fixed point $m \times m$ multiplication requires $O(m^2)$ cycles [12].

Floating point arithmetic for associative processors is difficult to implement. Different exponents require shifting mantissas by different lengths, resulting in a sequence of bit-serial operations. A direct implementation of IEEE single precision floating point multiplication requires 4400 cycles.

In general, any analytical equation can be efficiently implemented on an associative processor using a Look Up Table (LUT) approach, where all possible arguments of the function are matched vs. the content of the associative array, and the corresponding function values are written in the designated fields of the tagged memory rows. For a $m$-bit argument $x$, such $f(x)$ (no matter how complex it is) has $2^m$ possible values, therefore LUT operation costs $O(2^m) = 2^{m+1}$ cycles. Obviously, all values of the $f(x)$ LUT are pre-calculated and implicitly stored in the associative processor instructions.

As follows from TABLE 1, most of the data words (AP rows) are mismatched during arithmetic operations. Hence, the NOR-type AP cell is relatively inefficient power-wise because a mismatch results in discharging the Match line. Different AND-type AP cell designs have been proposed to reduce the power dissipation of the compare operation, possibly at the penalty of slower operation [13].

## 3 ANALYTIC MODEL AND COMPARATIVE ANALYSIS

In this section we develop an analytical performance model of the conventional SIMD and the associative processors and compare their relative performance, area and power consumption under constrained area and power

resource. Here we study only the parallelizable portion of a workload. For simplicity, we assume that the parallelizable portion contains single-cycle instructions (i.e. arithmetic, control, register file access and alike). We also assume the performance of the baseline sequential CPU to be 1 for the sake of estimating the relative speedup delivered by the reference SIMD coprocessor and the associative processors.

### 3.1 Reference SIMD Processor

Fig. 5 details the computer architecture comprising the sequential CPU, the shared LLC and the SIMD coprocessor, as depicted in Fig. 1(b). The reference SIMD coprocessor contains a number of baseline processing elements (BPEs), each containing a floating point ALU and a register file. The BPEs are connected to the shared LLC through a bandwidth-limited interface, and are interconnected using an interconnection network (not shown).

Let the serial execution time of the parallelizable portion $f$ of the program on the baseline sequential CPU be $T_1$. The execution time $T_{f,SIMD}$ of the same parallelizable portion on the SIMD coprocessor can then be written as follows:

$$T_{f,SIMD} = \frac{T_1}{n_{SIMD}} + \frac{T_C}{n_{SIMD}} + T_S \quad (1)$$

where $n_{SIMD}$ is the number of BPEs, $T_C$ is the time spent exclusively on inter-BPE communication, and $T_S$ is the time spent exclusively on synchronization of the LLC to the private SIMD memory (the register files of BPEs) [8]. The synchronization consists of the time to move data from LLC to SIMD before the parallel segment starts, and from SIMD to LLC after the parallel segment completes. Since it involves access to a shared resource, $T_S$ might depend on the number of BPEs in the SIMD coprocessor [14], [15]. This is especially the case when the data set size is scaled down to the processor size.

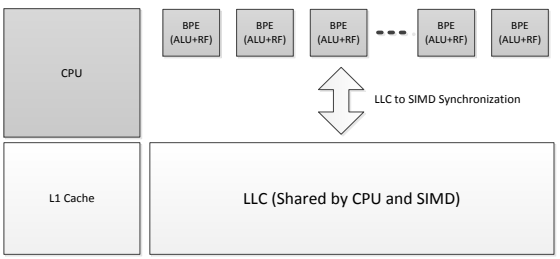


Fig. 5. CPU with SIMD coprocessor and shared LLC

While a number of BPEs (or all BPEs) can communicate with each other in parallel (although using a potentially congested interconnection network that affects $T_C$), the LLC-to-SIMD synchronization is done essentially serially for each BPE. Therefore the inter-BPE communication time scales by the number of BPEs while $T_S$ does not scale. The speedup of the SIMD processor over the sequential CPU can be written as follows:

$$S_{SIMD} = \frac{T_1}{T_{f,SIMD}} = \frac{T_1}{\frac{T_1}{n_{SIMD}} + \frac{T_C}{n_{SIMD}} + T_S} = \frac{1}{\frac{1}{n_{SIMD}} + \frac{I_c}{n_{SIMD}} + I_s} \quad (2)$$

where $I_c = T_C/T_1$ is the *connectivity intensity*, or ratio of the time spent on inter-BPE communication to the serial execution time, and $I_s = T_S/T_1$ is the *synchronization intensity*, or the ratio of time spent on LLC-to-SIMD synchronization to the serial execution time. Synchronization intensity (Fig. 6) inversely proportional to the arithmetic intensity, defined as the ratio of arithmetic operations to memory traffic [16], [17].

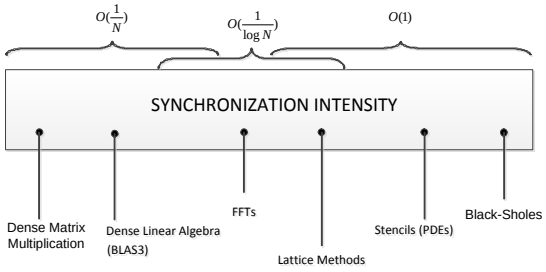


Fig. 6. Synchronization Intensity

While the cost of communication between the processing elements in terms of speedup impact (delay) and power is not negligible, in this study we assume $I_c = 0$. The reason for this assumption is as follows. While computation and LLC-to-SIMD synchronization in conventional SIMD and in associative processor are very different as we show below, the inter-PE communication could be similar and therefore can be omitted from the comparative analysis without significantly affecting the results.

The area of the SIMD processor can be presented as follows:

$$A_{SIMD} = n_{SIMD}(A_{ALU} + A_{RF}) \quad (3)$$

where $A_{ALU}$ is the ALU area and $A_{RF}$ is the register file area. As noted above, the inter-PE connection network is omitted.

For easy comparison between processing element and memory areas, we represent all area values (ALU, registers, memory) in terms of baseline SRAM cell area. Let the baseline SRAM cell area be 1. In current CMOS technology, the actual figure is in the range of $\sim 0.1\mu m^2$.Then we can write:

$$A_{ALU} = A_{ALUo}m^2 \quad A_{RF} = A_{RFo}km \quad (4)$$

where $A_{ALUo}$ is the area of a single bit of the ALU and $A_{RFo}$ is the area of a register bit (a flip-flop), both measured in baseline SRAM cell area units; $m$ is data wordlength and $k$ is the depth of the register file. This model is quite basic and does not take into account numerous aspects of BPE (such as instruction cache, communication and control).

Its purpose is providing the best case reference figures for the comparative analysis of the conventional SIMD processor's speedup, area and power.

The average power of the SIMD processor (over the execution span $T_{f,SIMD}$) can be written as follows:

$$P_{SIMD} = \frac{E_{EXEC} + E_S + E_{LEAK}}{T_{f,SIMD}}$$
$$= \frac{P_{EXEC} \cdot \frac{T_1}{n_{SIMD}} + P_S \cdot T_S + P_{LEAK} \cdot (\frac{1}{n_{SIMD}} + I_s) \cdot T_1}{(\frac{1}{n_{SIMD}} + I_s) \cdot T_1} \quad (5)$$
$$= \frac{\frac{P_{EXEC}}{n_{SIMD}} + I_s \cdot P_S}{(\frac{1}{n_{SIMD}} + I_s)} + P_{LEAK}$$

where $T_{f,SIMD}$ is the execution time of the parallelizable portion of the program on the SIMD processor (1); $E_{EXEC}$ and $P_{EXEC}$ are the energy and the average power consumption during execution; $E_S$ and $P_S$ are the energy and the average power consumed during LLC-to-SIMD synchronization; $E_{LEAK}$ and $P_{LEAK}$ are the leakage energy and power; $I_s$ is the synchronization intensity as defined above.

Just as in the case of area comparison, we represent all power values (ALU, registers, memory) through the power consumption of a baseline SRAM memory cell. Let the power consumption of the baseline SRAM cell during write be 1 (operation is bound by the memory array; there is no data transfer outside the memory). Then we can further write the SIMD power consumption as follows:

$$P_{EXEC} = n_{SIMD}(P_{ALUo}m^2 + P_{RFo}km)$$
$$P_S = P_{So}m \quad (6)$$

where $P_{ALUo}$ and $P_{RFo}$ are the average per-bit power consumptions of the ALU and RF respectively during execution (computation). $P_{So}$ is the power consumed performing LLC-to-SIMD synchronization of a single data bit. We assume the amount of data that needs to be synchronized with the shared last level memory is limited to a single data word per BPE (as typical in applications such as dense matrix multiplication and FFT). $P_{EXEC}$ and $P_S$ are measured in SRAM cell write power consumption units.

Leakage power can be expressed as follows:

$$P_{LEAK} = \beta A V^{\alpha} \quad (7)$$

where $A$ is the area, $V$ is the supply voltage, and α and β are constants. Therefore the total power can be written as follows:

$$P_{SIMD} = \frac{P_{ALUo}m^2 + P_{RFo}km + I_s P_{So} m}{\frac{1}{n_{SIMD}} + I_s} +$$
$$+\gamma \cdot n_{SIMD} \cdot (A_{ALUo}m^2 + A_{RFo}km) \quad (8)$$

where $\gamma = \beta V^{\alpha}$ is the leakage area coefficient that depends on process and operating conditions. Note that for comparison purposes we use the same leakage power (represented as a function of area only as in (7)) for both the associative processor and the SIMD processor. This might be somewhat unfair to the associative processor: First, the leakage power per area could be lower for memory than for logic [11]. Second, the associative processor has fewer hotspots. Since the leakage power is highly temperature dependent, hotspots may lead to higher leakage in the SIMD processor [6].

### 3.2 Associative Processor

In this section we construct the analytical model for the speedup, area and power consumption of the associative processor as per architecture depicted in Fig. 1(c). The execution time of the parallelizable portion $f$ of the program on associative processor can be written as follows:

$$T_{f,AP} = \frac{T_1}{s_{APE} n_{AP}} + \frac{T_C}{n_{AP}} \quad (9)$$

where $n_{AP}$ is the number of processing elements in the associative processor, $s_{APE}$ is the speedup of associative processing element relative to the baseline sequential CPU, and $T_C$ is as defined in (1). Since the associative processor replaces the LLC and combines data processing and data storage, there is no need for synchronization and therefore $T_s$ is omitted from (9).

Assuming single precision floating point arithmetic, the longest among frequently used arithmetic operations is multiplication, which in one direct implementation takes 4400 cycles vs. 1 cycle on the baseline sequential CPU or the BPE. Lacking *a-priori* knowledge of the workloads to be executed on the associative processor, we assume the worst case scenario comprising a continuous series of floating point multiplications. In this case $s_{APE} = 1/4400$. The speedup of the associative processor ($I_c$ is assumed to be zero, as discussed above) can then be written as follows:

$$S_{AP} = \frac{1}{\frac{1}{s_{APE} n_{AP}} + \frac{I_c}{n_{AP}}} = s_{APE} n_{AP} \quad (10)$$

The area of the associative processor can be written as follows:

$$A_{AP} = n_{AP} A_{APo} km \quad (11)$$

where $k$ is the size of associative processing element (in data words, same as the size of the SIMD BPE register file in (4)) and $A_{APo}$ is the associative processor cell area, measured in SRAM cell area units. Similarly to the reference SIMD coprocessor, we ignore the area of the interconnection network.

The average power of the associative processor can be written as follows:

$$P_{AP} = \frac{E_{EXEC} + E_{LEAK}}{T_{f,AP}} = P_{EXEC} + P_{LEAK} = [\frac{P_W + P_C}{2} + \gamma A_{APo} km] n_{AP} \quad (12)$$

Where $E_{EXEC}$ and $P_{EXEC}$ are the associative processor execution energy and power consumption; $E_{LEAK}$ and $P_{LEAK}$ are the associative processor leakage energy and power; $P_W$ is the power consumption during memory write operation and $P_C$ is the power consumption during compare operation (the activities, or the probabilities of compare and write in arithmetic operations are virtually equal (0.5)). In order to further detail the dynamic power of the associative processor, we revert to the implementation of the full bit adder (which is a building block of the other arithmetic operations) described in Sect. 1. Assuming the sum overwrites one of the summands, one bit addition takes four compare-and-write steps. In each step, a three bit input combination $A, B, C_{in}$ is compared and afterwards a two bit result $S, C_{out}$ is written, repeated $m$ times for $m$-bit words. Since there are eight independent logic combinations (TABLE 1), each processing element has $1/8$ probability of match and $7/8$ of mismatch (in which case the Match line discharges). Similarly, each processing element has $1/8$ probability of write and $7/8$ probability of a *miswrite* (when Bit and Bit' lines are charged without Word line being asserted). Since we defined the power consumption of SRAM cell during write operation as 1, (12) can be rewritten as:

$$P_{EXEC} = \frac{(2 \cdot 1/8 + 2 \cdot 7/8 \cdot p_{nw}) + (3 \cdot 1/8 \cdot p_m + 3 \cdot 7/8 \cdot p_{mm})}{2} n_{AP} \quad (13)$$

where $p_{nw}$ is the per-bit power consumption of a miswrite, $p_{mm}$ is the per-bit power consumption of a mismatch, and $p_m$ is the per-bit power consumption of a match, relative to the power consumption of SRAM cell during write operation.

Using (7), we can write the total power dissipation of the associative processor as follows:

$$P_{AP} = n_{AP} \cdot [\frac{2 \cdot 1/8 + 2 \cdot 7/8 \cdot p_{nw} + 3 \cdot 1/8 \cdot p_m + 3 \cdot 7/8 \cdot p_{mm}}{2} + \gamma A_{APo} km] \quad (14)$$

This model is fairly basic and does not account for certain statistics that work in favor of the associative processor. For example, a certain percentage of memory cells that are written a new value in fact do not change; similarly, a certain percentage of asserted bit lines do not recharge (or discharge) since the same value is asserted; ~1/8 of Match lines consume very little power during precharge because the last compare was a match and the Match line did not discharge. Our goal is to create a simple power model that reflects the worst case power consumption of the associative processor.

### 3.3 Modeling under constrained area

In this section, we compare the speedup of the associative processor *vs.* the reference SIMD coprocessor subject to the constrained total area budget $A$ for either processor. We can derive the number of BPEs $n_{SIMD}$ as the function of the total area of the SIMD coprocessor using (3) and (4) as follows:

$$n_{SIMD} = \frac{A}{A_{ALU} + A_{RF}} = \frac{A}{A_{ALUo} m^2 + A_{RFo} km} \quad (15)$$

We assume $A_{ALUo}, A_{RFo}, k$ and $m$ are constant and are not functions of the area budget. We further substitute $n_{SIMD}$ in (2) and (5) by (15) and receive the speedup and the power consumption of the reference SIMD coprocessor as function of the area budget.

As for the associative processor, the number of its processing elements may be derived as the function of the associative processor area using (11) as follows:

$$n_{AP} = \frac{A}{A_{APo} km} \quad (16)$$

where $A$ is the same constrained area budget as in (15). We can now substitute $n_{AP}$ in (10) and (13) by (16) and obtain the speedup and the power consumption of the associative processor as function of the area budget. The area parameters we use for modeling purposes are presented in TABLE 2.

Speedup vs. area for the reference SIMD coprocessor and the associative processor is shown in Fig. 7. Synchronization intensity $I_s$ is assumed to be 0.01 (namely, synchronization takes 1% of the serial execution time).

TABLE 2
AREA MODEL PARAMETERS

| Parameter | Description | Attributed to | Value |
|---|---|---|---|
| $A_{ALUo}$ | ALU bit cell area | SIMD | 20 (1) |
| $A_{RFo}$ | Register bit (FF) area | SIMD | 3 (1) |
| $S_{APE}$ | AP speedup relative to sequential CPU | AP | 1/4400 |
| $A_{APo}$ | AP bit area | AP | 2 (1) |
| $m$ | Data wordlength | Both | 32 |
| $k$ | Number of data words in temporary storage | Both | 8 |

*(1) Area parameters are relative to the area of SRAM bit cell*

As the area budget increases, the speedup of the reference SIMD coprocessor exhibits diminishing returns caused by the delay of synchronizing LLC-to-SIMD private memory. Eventually the speedup saturates [8]:

$$\lim_{n_{SIMD} \to \infty} S_{SIMD} = \lim_{n_{SIMD} \to \infty} \frac{1}{\frac{1}{n_{SIMD}} + I_s} = \frac{1}{I_s} \quad (17)$$

This effect does not exist in the associative processor since LLC-to-SIMD synchronization is not required. As evident from Fig. 7, the speedup of the associative proces-

sor is lower than the reference SIMD coprocessor at low area, but it rises linearly with area because it is unaffected by LLC-to-SIMD synchronization. The breakeven point occurs at around $\sim 20mm^2$.

The power consumption vs. area budget for the SIMD and the associative processors is shown in Fig. 8. The power consumption of the associative processor is lower than that of the SIMD processor when area is under $\sim 38mm^2$. For larger area, the associative processor consumes more power than the SIMD processor. The area range of $\sim 20mm^2$ to $\sim 38mm^2$ might be a sweet spot for the associative processor as it may outperform the SIMD processor while at the same time consuming less power. Note that even when the speedup of the SIMD processor saturates, its power consumption continues to grow with area, due to power consumed by LLC-to-SIMD synchronization as well as the leakage power of the SIMD processor.

The performance/power ratio vs. area for the SIMD and the associative processors is shown in Fig. 9. For the associative processor, the performance is proportional to power consumption. For the SIMD processor, the performance/power ratio drops because speedup saturates while power dissipation continues to grow with increasing area.

The energy-delay product ($ED$) vs. area for the SIMD and the associative processors is shown in Fig. 10. The SIMD processor's $ED$ reaches a minimum around $\sim 5mm^2$ (where the speedup saturates) and begins to grow again due to growing power consumption. The associative processor's $ED$ is inversely proportional to the processor size, and therefore monotonically decreasing with growing area. It begins to outperform the SIMD processor when area reaches $\sim 17mm^2$.

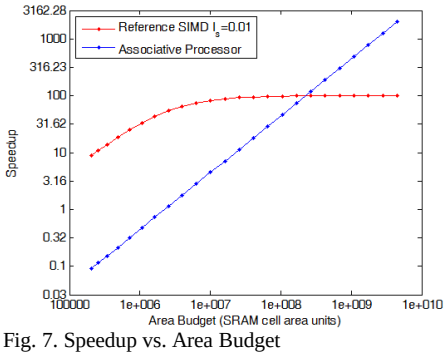

Fig. 7. Speedup vs. Area Budget

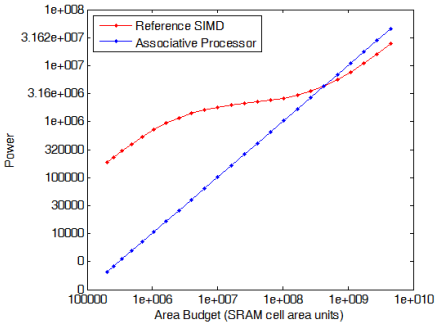

Fig. 8. Power Consumption vs. Area Budget

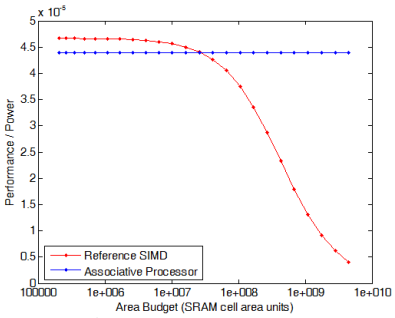

Fig. 9. Performance / power ratio vs. Area Budget

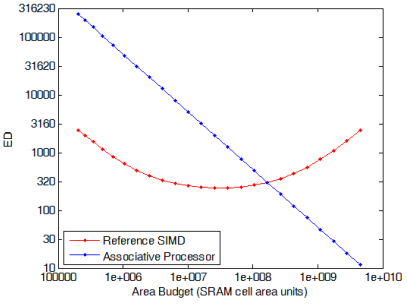

Fig. 10. $ED$ vs. Area Budget

### 3.4 Modeling under constrained power

In this section, we compare the speedup of the associative and reference SIMD coprocessors subject to constrained power budget. We can derive the number of BPEs in the SIMD processor as the function of the power budget by solving (8) for $n_{SIMD}$, which leads to the following quadratic equation:

$$a{n_{SIMD}}^2 + bn_{SIMD} + c = 0 \tag{18}$$

where

$$a = I_s\gamma(A_{ALUo}m^2 + A_{RFo}km)$$
$$b = P_{ALUo}m^2 + P_{RFo}km + I_sP_{So}m +$$
$$+\gamma(A_{ALUo}m^2 + A_{RFo}km) - I_sP$$
$$c = -P$$
$$n_{SIMD} = \frac{\sqrt{b^2 - 4ac} - b}{2a} \tag{19}$$

and where $P$ is the constrained power budget. We can further substitute $n_{SIMD}$ in (2) and (3) by (19) and estimate the speedup and the area of the reference SIMD coprocessor under the constrained power dissipation budget.

The number of processing elements of the associative processor can be derived as the function of the associative processor power budget by solving (14) for $n_{AP}$ as follows:

$$n_{AP} = \frac{P}{\frac{2{\cdot}1/_8 + 2{\cdot}7/_8{\cdot}p_{nw} + 3{\cdot}1/_8{\cdot}p_m + 3{\cdot}7/_8{\cdot}p_{mm}}{2} + \gamma A_{APo}km} \tag{20}$$

where $P$ is the same constrained power budget as in (19). We can now substitute $n_{AP}$ in (10) and (11) by (20) and obtain the speedup and the area of the associative processor as function of the power budget. The parameters used

for modeling are presented in TABLE 3.

The speedup vs. power budget for the two processors is shown in Fig. 11. The speedup of the reference SIMD coprocessor is affected by diminishing returns caused by LLC-to-SIMD synchronization, while the speedup of the associative processor grows proportionally to the power budget (see (20) and (10)). The area vs. power is shown in Fig. 12, the performance/power ratio is shown in Fig. 13, and the energy-delay product ($ED$) is shown in Fig. 14.

TABLE 3
POWER MODEL PARAMETERS

| Parameter | Description | Attributed to | Value |
|---|---|---|---|
| $P_{ALUo}$ | per-bit power consumption of ALU | SIMD | 20 (1) |
| $P_{RFo}$ | per-bit power consumption of RF | SIMD | 3 (1) |
| $P_{So}$ | per-bit power consumption during synchronization | SIMD | 200 (1) |
| $p_{nw}$ | per-bit power consumption during a miswrite | AP | 0.75 (1) |
| $p_m$ | per-bit power consumption during a match | AP | 1 (1) |
| $p_{mm}$ | per-bit power consumption during a mismatch | AP | 1.25 (1) |
| $\gamma$ | static power coefficient | Both | $5 \cdot 10^{-3}$ (2) |

*COMPARE and WRITE are executed within the AP array; there is no data transfer outside the AP memory*

(1) *Power parameters are relative to the power consumption of SRAM bit cell during write operation*

(2) *Power consumption of SRAM bit cell unit over area of SRAM bit cell unit*

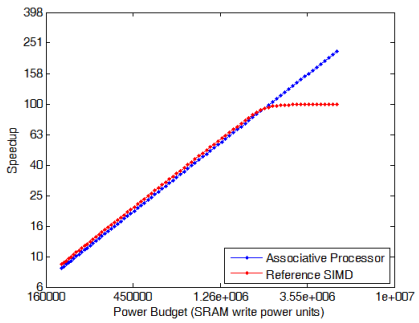

Fig. 11. Speedup vs. Power Budget

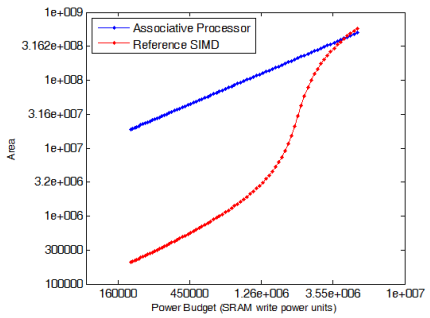

Fig. 12. Area vs. Power Budget

## 3.5 Sensitivity to parameter variation

The parameters used in our modeling (TABLE 2 and TABLE 3) are technology and architecture dependent and therefore may change with feature size, design style etc. In order to determine how the changes in these parameters affect the results, we randomize the parameters in TABLE 2 and TABLE 3 using uniform distribution of $\mp 50\%$.

Fig. 15 shows the distribution of the speedup breakeven point (i.e. the area at which the speedup of the SIMD processor is the same as that of the associative processor, $\sim 20mm^2$ in Fig. 7). As expected, the distribution of speedup breakeven point is close to lognormal (because at least some of the independent random parameters are positive and multiplicative), with a mean value of $\sim 22mm^2$.

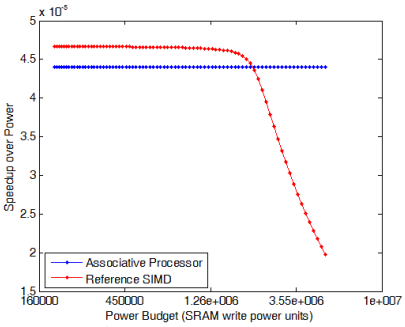

Fig. 13. Performance / Power Ratio vs. Power Budget

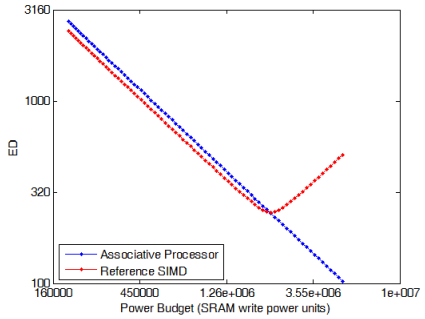

Fig. 14. $ED$ vs. Power Budget

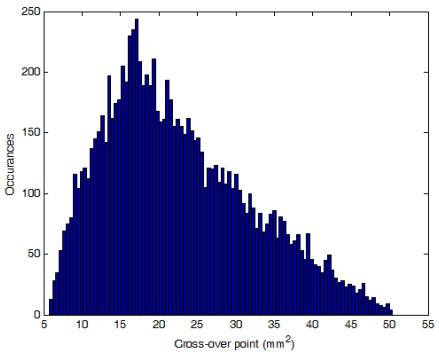

Fig. 15. Speedup Breakeven Points Distribution

## 3.6 Speedup Simulation

The purpose of the simulation is to validate the analytic results obtained in Sections 3.3 and 3.4. The workloads are defined, followed by description of the results.

### 3.6.1 Workloads

The workloads selected for performance and power consumption simulations are as follows:

- $N$-option pairs Black-Sholes pricing (single preci-

sion floating point)

- $N$-point Fast Fourier Transform (FFT, Radix 2, single precision floating point)
- Dense Matrix Multiplication of two $\sqrt{N}\times\sqrt{N}$ matrices (single precision floating point)

where $N$ is the data set size, scaled to the size of the processor. The LLC-to-SIMD synchronization is the main reason for the speedup limitation of the conventional SIMD coprocessor relative to the associative processor. These workloads are therefore significant because they span the wide range of synchronization intensities (Fig. 6).

For dense matrix multiplication and FFT, we used optimized implementations outlined in [18]. For Black-Scholes, we used a direct implementation optimized for associative processing, based on formulation in [19].

### 3.6.2 Results

We simulate speedup, power and performance/power ratio per workload for a wide range of area budget, similarly to Section 3.3.

Fig. 16 presents the synchronization intensity $I_s$ as function of area budget and data set size for each workload. While in the analytical model we use constant synchronization intensity, different workloads come with different $I_s$. The synchronization intensity for Black-Scholes option pricing is $I_s = 0.02$ and does not change with the data set size. The synchronization intensity for FFT is $I_s = O(1/\log N)$ and thus it decreases mildly with the data set size. The synchronization intensity for DMM is $I_s = O(1/N)$, dropping quickly with data size.

The results of speedup vs. area simulation are presented in Fig. 17. They are similar to the analytical model as depicted in Fig. 7. The differences in simulation behavior are the result of the differences in synchronization intensity of each individual workload. While for the associative processor, speedup is proportional to the processor size (area) for all three workloads, the relation between the speedup and the processor size for the reference SIMD coprocessor is different. Since Black-Sholes's synchronization intensity is at the higher end of the scale (Fig. 6), the LLC-to-SIMD synchronization delay is relatively significant, and the speedup of SIMD processor saturates relatively quickly just under $1/0.02 = 50$ (see (17)). The speedup breakeven point for Black-Sholes option pricing lies at around $\sim 10mm^2$.

FFT's synchronization intensity is in the middle of the range, so that the LLC-to-SIMD synchronization delay is less significant. The speedup of the SIMD processor continues to slightly grow, as its synchronization intensity decreases with the area and the data set size. The speedup breakeven point is at around $\sim 7.5mm^2$.

Synchronization intensity for dense matrix multiplication is at the lower end of the range, so that the LLC-to-SIMD synchronization delay is relatively negligible, and the speedup of SIMD processor does not saturate and continues to grow, although at a slower pace than the speedup of the associative processor. The speedup breakeven point is at around $\sim 8mm^2$.

Note that in more realistic scenario, where the data set size and the task size are constant rather than scaled to the processor size, the synchronization intensity is also constant and so the simulated speedup is identical to the analytic model for all there workloads.

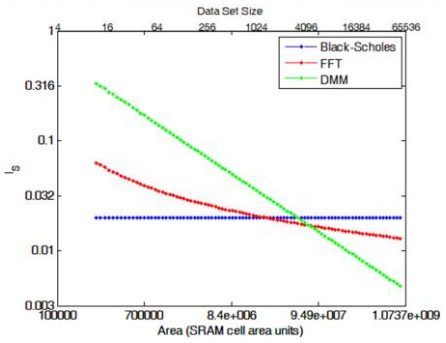


Fig. 16. Synchronization Intensity $I_s$ vs. Area and Data Set Size

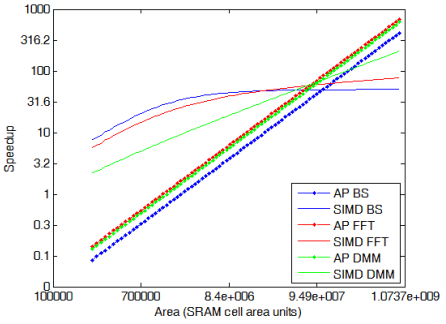


Fig. 17. Simulated Speedup vs. Area

The power consumption vs. area results are presented in Fig. 18. These results are in line with the analytical model as depicted in Fig. 8, except for the dense matrix multiplication where the simulated synchronization intensity is quite different from the analytical model. The performance/power ratio vs. area results are presented in Fig. 19. Similarly, the results resemble the analytical model as depicted in Fig. 9. Thus, the simulations validate the analytic models of Sections 3.3 and 3.4.

## 4 CPU WITH ASSOCIATIVE PROCESSOR VS. CPU WITH LLC AND SIMD COPROCESSOR

While in the previous sections the associative processor has been compared with a standalone SIMD processor, in this section they are considered in the context of a complete CPU system. We compare the performance and power of a CPU with either an associative processor (Fig. 1(c)), or with a LLC and a conventional SIMD coprocessor (Fig. 1(b)), both under constrained area resource. In this analysis we assume that the areas of the CPU and the L1 cache are constant. The variable area budget is therefore assigned entirely to the LLC in the baseline architecture (Fig. 1(a)), or divided among the LLC and the SIMD coprocessor (Fig. 1(b)), or assigned entirely to the associative processor (Fig. 1(c)). In the SIMD coprocessor analysis, we assume synchronization intensity $I_s = 0.01$ similarly to the Section 3.3. We begin our comparative analysis with performance and follow with power consumption.

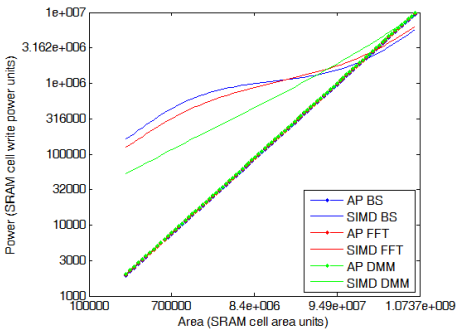

Fig. 18. Simulated Power Consumption vs. Area

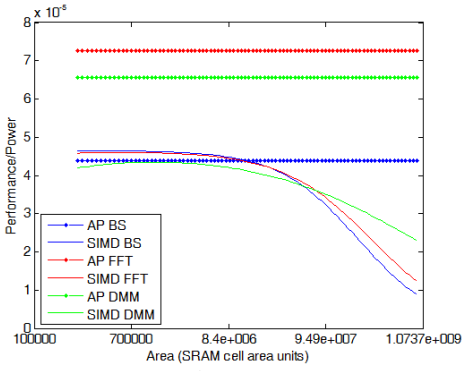

Fig. 19. Simulated Performance / power ratio vs. Area

### 4.1 Performance

Following [20] and [21], we can present the execution time of a workload on the baseline CPU architecture (Fig. 1(a)) as a function of its LLC size $A_{LLC} = A$ as follows:

$$T_1(A_{LLC}) = M[g \cdot CPI_{MEM} + (1-g) \cdot CPI_{CPU}] \tag{21}$$

where $A$ is the area budget, $M$ is the number of instructions in the workload, $g$ is the fraction of memory access instructions, $CPI_{CPU}$ is the average number of cycles per instruction for instructions that require no memory access (assumed to be constant, as defined in TABLE 4), and $CPI_{MEM}$ is the average number of cycles per memory access. $CPI_{MEM}$ can be further presented as follows:

$$CPI_{MEM} = (1-m_1)d_{L1} + m_1(1-m_2)d_{LLC} + m_1 m_2 d_D \tag{22}$$

where $m_1$ and $m_2$ are miss rates of L1 and LLC respectively, $d_{L1}$ and $d_{LLC}$ are access times of L1 and LLC respectively, and $d_D$ is the off-chip DRAM access time.

The miss rate of the LLC can be written as follows [22]:

$$m_2 = m_1\sqrt{A_{L1}/A_{LLC}} \tag{23}$$

where $A_{L1}$ and $A_{LLC} = A$ are the areas of the L1 and the LLC respectively.

The execution time of the same workload on the CPU with the LLC and the SIMD coprocessor can be written as follows:

$$T_2 = (1-f) \cdot T_1(A_{LLCo}) + \frac{f \cdot M}{s_{SIMD}(A_{SIMDo})} \tag{24}$$

where $f$ is the parallelizable portion of the program and $s_{SIMD}$ is the speedup of the SIMD coprocessor as defined in (2); $A_{LLCo}$ and $A_{SIMDo}$ are the optimal areas of the LLC and the SIMD coprocessor, respectively, so that $A_{LLCo} + A_{SIMDo} = A$. The parallelizable portion of the workload is assumed to contain single-cycle instructions, similarly to Section 3.

Although this is out of the main focus of our analysis, we minimize $T_2$ by optimally dividing the area budget between the LLC and the SIMD coprocessor, through numerically solving the following equation for $A_{LLC}$ (the optimal result is $A_{LLCo}$):

$$\frac{\partial T_2}{\partial A_{LLC}} = \frac{\partial}{\partial A_{LLC}}\left[(1-f) \cdot T_1(A_{LLC}) + \frac{f \cdot M}{s_{SIMD}(A - A_{LLC})}\right] = \\ = -0.5M(1-f)(1-g)m_1^2(d_D - d_{LLC})\sqrt{A_{L1}}A_{LLC}^{-\frac{3}{2}} \\ + \frac{(A_{ALU} + A_{RF})Mf}{A^2 - 2A_{LLC}A + {A_{LLC}}^2} = 0; \tag{25}$$

where $(A_{ALU} + A_{RF})$ is the size of SIMD coprocessor's BPE as defined in (3). The optimal SIMD coprocessor area $A_{SIMDo}$ can then be found as follows:

$$A_{SIMDo} = A - A_{LLCo} \tag{26}$$

The execution time of the same workload on the CPU with the associative processor can be written as:

$$T_3 = (1-f) \cdot T_1(A/A_{APo}) + \frac{f \cdot M}{S_{AP}} \tag{27}$$

where $S_{AP}$ is the speedup of the associative processor as defined in (10); $A/A_{APo}$ is the effective area of the LLC implemented by the associative processor (operated in the conventional cache mode during the execution of the serial portion of the workload), where $A_{APo}$ (the area of the associative processor cell in SRAM cell units) is 2, as defined in TABLE 2.

Following (24) and (27), the effective number of cycles per instruction for the CPU with the LLC and the SIMD coprocessor (Fig. 1(b)) and for the CPU with the associative processor (Fig. 1(c)) can be written as follows:

$$CPI_{SIMD} = \frac{T_2}{M}; \qquad CPI_{AP} = \frac{T_3}{M} \tag{28}$$

We further define the overall speedup of these two architectures as follows:

$$SU_{SIMD} = \frac{T_1(A)}{T_2}; \qquad SU_{AP} = \frac{T_1(A)}{T_3} \tag{29}$$

The timing and area parameters used for modeling purposes are specified in TABLE 2 and TABLE 4.

TABLE 4
TIMING AND AREA MODEL PARAMETERS

| Parameter | Description | Attributed to | Value |
|---|---|---|---|
| $g$ | fraction of memory access instructions | All | 0.2 |
| $CPI_{CPU}$ | average number of cycles per instruction for instructions that require no memory access | All | 1 |
| $A_{CPU}$ | CPU area | All | $10^8$ (1) |
| $A_{L1}$ | L1 cache area | All | $10^8$ (1) |
| $d_{L1}$ | L1 cache access time | All | 1 (2) |
| $d_{LLC}$ | LLC access time | All | 5 (2) |
| $d_D$ | DRAM access time | All | 100 (2) |
| $m_1$ | L1 cache miss rate | All | 0.05 |

*(1) Area parameters are relative to the area of SRAM bit cell*

*(2) Timing parameters are in cycles*

The optimal values of $A_{SIMD}$ and $A_{LLC}$ for the CPU with the LLC and the SIMD coprocessor, alongside the effective LLC size in the CPU with the associative processor for $f = 0.75, 0.9, 0.99$ and $0.999$, are shown in Fig. 20. The optimal values of $A_{SIMD}$ and $A_{LLC}$ for the SIMD accelerated architecture are calculated by solving (25) for each value of the constrained area budget $A$ (Fig. 20, horizontal axis). That area budget is divided between the LLC and the SIMD coprocessor, so the sum of red and black curves equals to the area budget at each point. For the CPU with the associative processor architecture, the entire area budget is assigned to the associative processor, so that the effective LLC size is $A/A_{APo}$ (blue curve). We assume inclusive cache, therefore the area budget starts at $A_{APo} \cdot A_{L1}$, so that the minimal effective LLC size in Fig. 1(c) architecture is $A_{L1}$. Note how the optimal area of the SIMD processor grows with $f$ relatively to the optimal area of the LLC, to eventually exceed it at $f = 0.999$.

Fig. 21 shows the effective number of cycles per instruction vs. area budget for both architectures for $f = 0.75, 0.9, 0.99$ and $0.999$. Fig. 22 shows the overall speedup of these architectures for the same $f$.

In Section 3 we established that the performance of the SIMD coprocessor is limited by the LLC-to-SIMD synchronization, so given large enough area budget and data set, the associative processor eventually outperforms the SIMD coprocessor. This outcome is supported by our findings here. For high $f$ (e.g., 0.9 and above), the effective CPI and overall speedup breakeven points occur at relatively low area budget, and the overall speedup is relatively high. For lower $f$ (e.g., 0.75 and below), the data set size and the area budget required for the associative processor to outperform the SIMD coprocessor are considerably more significant.

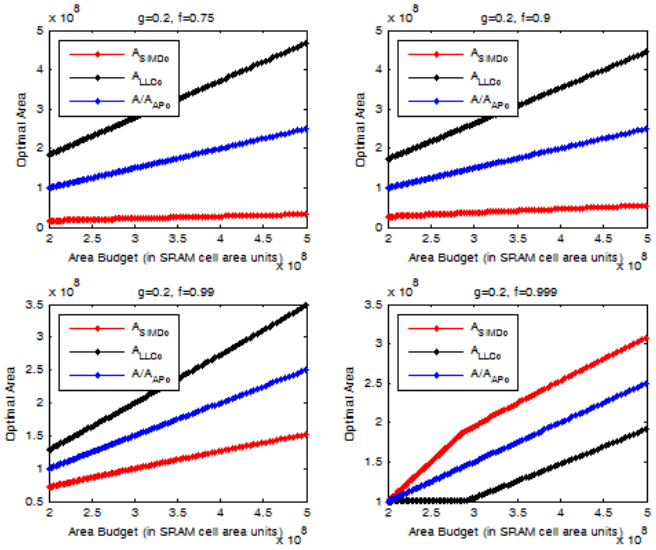


Fig. 20. Optimal area allocation vs. total area $A$

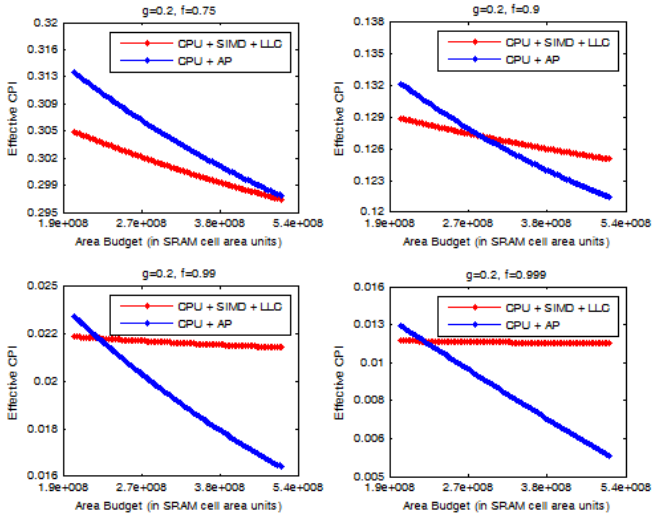


Fig. 21. Effective $CPI_{SIMD}$ and $CPI_{AP}$ vs. Area

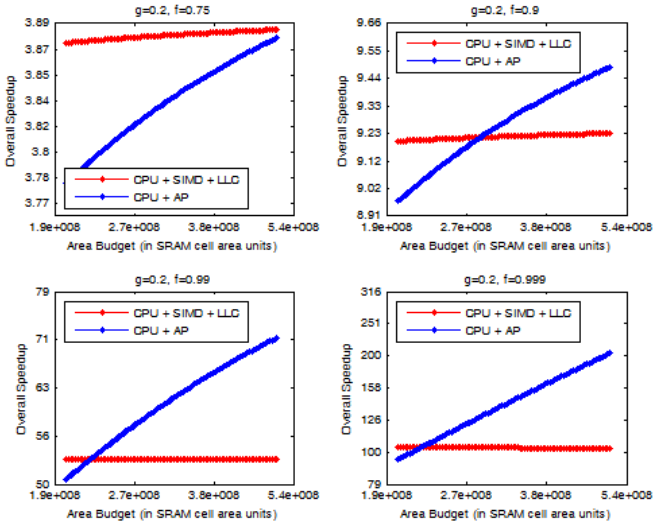


Fig. 22. $SU_{SIMD}$ and $SU_{AP}$vs. Area

### 4.2 Power Consumption

The power consumption of the baseline architecture in Fig. 1(a) can be presented as a function of its LLC size $A_{LLC} = A$ based on [23]:

$$P_1(A_{LLC}) = g \cdot P_{MEM} + (1-g) \cdot P_{CPU} + P_{LEAK} \quad (30)$$

where $P_{MEM}$ can be written as follows:

$$P_{MEM} = (1-m_1)P_{L1} + m_1(1-m_2)P_{LLC} + m_1 m_2 P_D \quad (31)$$

where $P_{L1}$, $P_{LLC}$ and $P_D$ are the power consumption of L1 cache, LLC, and off-chip DRAM access, respectively. $P_{L1}$ is assumed to be constant and defined in TABLE 5 below; $P_{LLC}$ to $P_{L1}$ ratio equals the square root of the LLC to L1 areas ratio, while $P_{CPU}$ is proportional to the CPU area [20]:

$$P_{LLC} = P_{L1} \cdot \sqrt{A_{LLC}/A_{L1}}; \qquad P_{CPU} = P_{CPUo} \cdot A_{CPU} \quad (32)$$

where $P_{CPUo}$ is the power consumption of the baseline CPU, assumed to be constant and defined in TABLE 5 below.

The power consumption of the CPU with the LLC and the SIMD coprocessor can be written as:

$$P_2 = (1-f) \cdot P_1(A_{LLCo}) + f \cdot P_{SIMD}(A_{SIMDo}) + P_{LEAK} \quad (33)$$

where $P_{SIMD}$ is the power dissipation of the SIMD coprocessor, which is the dynamic component of (5) above. The leakage power $P_{LEAK}$ is defined in (7) above (with $A$ being the sum of $A_{CPU}, A_{L1}, A_{SIMD}$ and $A_{LLC}$).

The power consumption of the CPU with the associative processor can similarly be written as follows:

$$P_3 = (1-f) \cdot P_1(A/A_{APo}) + f \cdot P_{AP} + P_{LEAK} \quad (34)$$

where $P_{AP}$ is the power dissipation of the associative processor, as defined in (13) above. The leakage power $P_{LEAK}$ is defined in (7) above (with $A$ being the sum of $A_{CPU}, A_{L1}$ and $A_{AP}$). The power parameters used for modeling are presented in TABLE 3 and TABLE 5.

TABLE 5
POWER MODEL PARAMETERS

| Parameter | Description | Attributed to | Value |
|---|---|---|---|
| $P_{CPUo}$ | Baseline CPU power | All | $5 \cdot 10^{-3}$ (1) |
| $P_{L1}$ | L1 power consumption | All | $5 \cdot 10^{4}$ (2) |
| $P_D$ | Power consumption during off-chip DRAM access | All | $10^{3}$(2) |

(1) *Power consumption of SRAM bit cell unit over area of SRAM bit cell unit*

(2) *Power parameters are relative to the power consumption of SRAM bit cell during write operation*

The power consumption, the performance/power ratio and the $ED$ product of the CPU with the LLC and the SIMD coprocessor vs. the CPU with the associative processor for $f = 0.75, 0.9, 0.99$ and $0.999$ are shown in Fig. 23, Fig. 24 and Fig. 25, respectively. Similarly to speedup, the results for higher $f$ are in line with the findings of Section 3.3. The power breakeven points for the two architectures lie above the effective $CPI_{AP}$ vs. $CPI_{SIMD}$ breakeven points of Fig. 21. This effect is more predominant for $f$ close to 1.

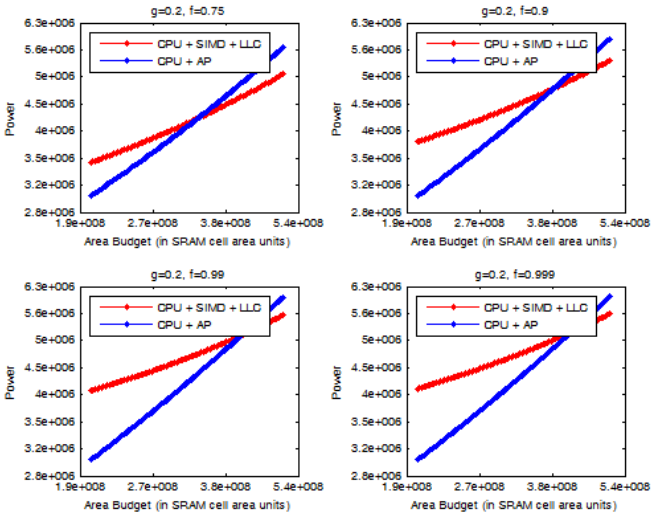


Fig. 23. Power vs. Area

Note the significant difference in behavior of the performance/power ratio and the $ED$ product for higher values of $f$. While at lower $f$ the associative processor consumes a large portion of the overall power while making small contribution to the overall speedup, for higher $f$ the associative processor adds to the overall speedup quite significantly. Consequently, for $f$=0.999, the CPU with the associative processor charts exhibit a trend completely different than the CPU with the LLC and the SIMD curves.

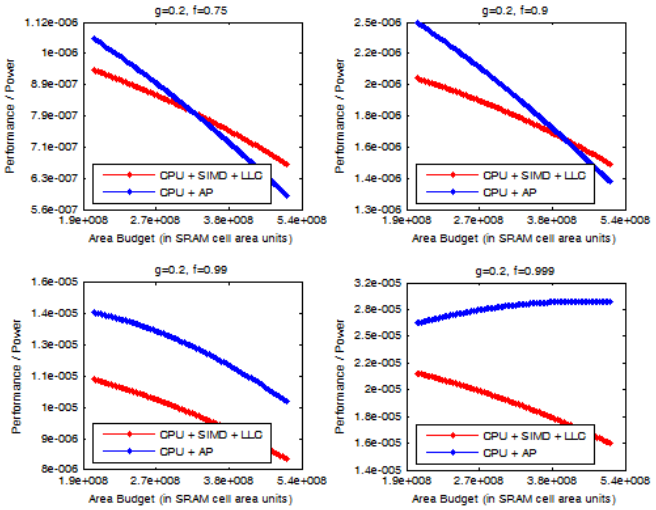


Fig. 24. Performance / Power vs. Area

Fig. 26 shows the effective $CPI_{AP}$ vs. $CPI_{SIMD}$ breakeven point, namely the area above which the CPU with the associative processor outperforms the CPU with the LLC and the SIMD, as a function of $f$ and $g$. The plateau

marks the region of $f$ and $g$ values for which a breakeven point cannot be achieved under the maximum area budget used in our analysis ($8A_{L1}$). In other words, the CPU with the associative processor does not have enough area to outperform the CPU with the LLC and the SIMD coprocessor. However, the SIMD processor is also less than useful in the plateau region: it is well established that conventional SIMD accelerators are inefficient in implementing low parallelizable / low arithmetic intensity workloads, characteristic of low $f$ and high $g$ (the plateau region) [4], [5].

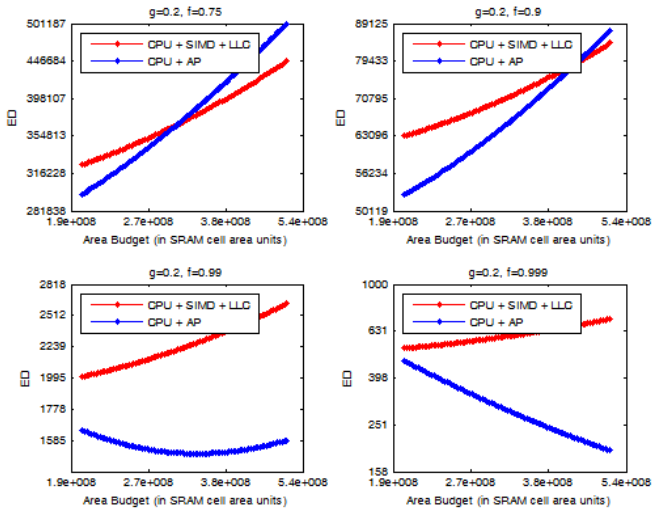


Fig. 25. $ED$ vs. Area

On the other hand, the combination of $f$ close to 1 and low $g$, which is typical for highly parallelizable compute-bound workloads with high arithmetic intensity, is highly advantageous for the CPU with the associative processor architecture, allowing it to outperform the SIMD accelerated architecture over the entire span of the area budget.

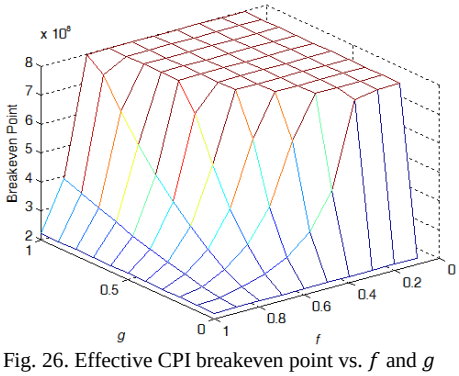


Fig. 26. Effective CPI breakeven point vs. $f$ and $g$

## 5 Discussion and Conclusions

An associate processor is essentially a large memory with massively-parallel processing capability. It offers dual use: either the CPU accesses the data in that memory, or the data is being processed associatively within the same memory. This paper investigates the merit of using associative processors instead of on-chip last level cache (LLC) combined with a SIMD accelerator.

Converting LLC into the associative processor adds parallel processing capabilities to otherwise sequential architecture. The price of this conversion is the reduction (approximately halving) of the effective LLC size in its conventional sequential processing mode. However, our study shows that even for workloads with relatively low parallelism ($f \leq 0.75$), replacing the LLC by the associative processor leads to an overall speedup over the baseline CPU architecture. For $f$ close to 1, such speedup can be quite significant.

An alternative way of improving the performance of parallelizable workloads is to allocate some of the constrained area budget (originally assigned to the LLC) to a conventional SIMD coprocessor. This study shows that the speedup of SIMD coprocessor is ultimately limited by massive data transfers between its private memory and the shared LLC. Aggressive multithreading, as discussed in [23], cannot completely resolve this bottleneck, unless there is an infinite supply of endless threads, since every new thread is likely to access data located in the shared memory. In other words, the LLC-to-SIMD synchronization is an unavoidable part of SIMD parallel execution, and there is no efficient way to eliminate its effect on speedup. This effect becomes more significant as the data set size and the SIMD coprocessor size grow.

The crucial advantage of the associative processor is the unification of data storage and data processing. Performance of the associative processor grows linearly with its size (area budget) since it is not impaired by data synchronization. Consequently, when the area budget (and the corresponding data set size) is large enough, the associative processor outperforms the conventional SIMD processor. The speedup breakeven point is in the area range of a few square millimeters to low tens of square millimeters depending on the workload, the feature size, the design specifics, etc.

Power consumption of the associative processor grows linearly with its size and generally follows the speedup pattern: the associative processor may consume more power than the SIMD processor above the speedup breakeven point. Yet, the associative processor seems to strongly outperform the conventional SIMD in terms of performance/power ratio and energy-delay product over a broad spectrum of area and power budget when the parallelism factor $f$ is close to 1.

Associative processing has been known and extensively studied since the 1960s. Commercial associative processing never quite took off, because only limited amounts of memory could be placed on a single die [24]. Due to data sets and tasks of limited size, a standalone bit- and word-parallel SIMD significantly outperformed associative processors. However, semiconductor technology has made the following progress in recent years, opening the door for reconsidering associative processors:

- Computational capabilities (and so the data set sizes) have grown significantly, e.g. from video compression of small frames at low frame rates to ultra-HD resolution at very high frame rates, and from communicating at telephone-rates to extensive switching

of massive bandwidth channels today. The paper shows that associative processing yields higher performance on large data sets.

- Power consumption, which used to be a secondary factor in the past, has grown to become a principal limitation to integration and performance today. The associative processor is shown to achieve higher performance/power ratios.
- While Moore's law continues to be maintained and transistor density continues to increase, the bandwidth of processors to memories is still limited. Associative processing mitigates that limitation because computing is intertwined with data storage.
- In high performance dies, power density is becoming the limit on total computation capabilities; associative processing leads to highly uniform power and thermal distribution over the chip area, avoiding hot spots and enabling higher power dissipation.

In addition to these technological aspects, associative processing architecture eliminates the synchronization bottlenecks of SIMD processors, thanks to *in-memory computing*.

## ACKNOWLEDGMENT

This research was partially funded by the Intel Collaborative Research Institute for Computational Intelligence.

## REFERENCES

[1] M. Gschwind, H.P. Hofstee, B.K. Flachs, M. Hopkins, Y. Watanabe, T. Yamazaki, "Synergistic processing in Cell's multicore architecture", IEEE Micro 26 (2), 2006, pp. 10–24

[2] "The Intel® Xeon Phi™ Coprocessor". Available at: http://www.intel.com/content/www/us/en/high-performance-computing/high-performance-xeon-phi-coprocessor-brief.html

[3] http://www.arm.com/products/processors/technologies/neon.php

[4] J. Owens *et al.*, "GPU Computing," Proceedings of the IEEE, Vol. 96, No. 5, pp. 879-899, May 2008

[5] David Luebke, "General-purpose computation on graphics hardware", Workshop, SIGGRAPH, 2004

[6] K. Banerjee et al., "A self-consistent junction temperature estimation methodology for nanometer scale ICs with implications for performance and thermal management," IEEE IEDM, 2003, pp. 887-890.

[7] S. Borkar. "Thousand Core Chips: A Technology Perspective," *Proc. ACM/IEEE 44th Design Automation Conf. (DAC)*, 2007, pp. 746-749.

[8] L. Yavits, A. Morad, R. Ginosar, "The effect of communication and synchronization on Amdahl's law in multicore systems", CCIT Report #814, 2012, http://webee.technion.ac.il/publication-link/index/id/611.

[9] I. Scherson, Kramer, Alleyne, "Bit-Parallel Arithmetic in a Massively-Parallel Associative Processor", IEEE Transactions on Computers, Vol. 41, No. 10, October 1992

[10] Yau, Fung, "Associative Processor Architecture - a Survey", ACM Computing Surveys Journal (CSUR), Volume 9, Issue 1, March 1977, Pages 3 – 27

[11] F. Pollack, "New microarchitecture challenges in the coming generations of CMOS process technologies (keynote address)", MICRO 32, 1999

[12] C. Foster, "Content Addressable Parallel Processors", Van Nostrand Reinhold Company, NY, 1976

[13] H.-Y. Li, C.-C. Chen, J.-S. Wang, and C. Yeh, "An AND-type match line scheme for high-performance energy-efficient content addressable memories," IEEE Journal of Solid-State Circuits , vol. 41, no. 5, pp. 1108 – 1119, May 2006.

[14] B. Rogers, A. Krishna, G. Bell, K. Vu, X. Jiang, Y. Solihin, "Scaling the Bandwidth Wall: Challenges in and Avenues for CMP Scaling". In ISCA '09: Proceedings of the 36th annual international symposium on Computer architecture, pages 371–382, New York, NY, USA, 2009. ACM

[15] H. Flatt., K. Kennedy "Performance of Parallel Processors," Parallel Computing, Vol. 12, No. 1, 1989, pp. 1-20.

[16] S. Kamil, C. Chan, L. Oliker,, J. Shalf, S. Williams, "An Auto-Tuning Framework for Parallel Multicore Stencil Computations", IEEE International Symposium on Parallel & Distributed Processing (IPDPS) 2010, pages 1-12.

[17] S. Williams, D. Patterson, L. Oliker, J. Shalf, K. Yelick, "The roofline model: A pedagogical tool for auto-tuning kernels on multicore architectures," Hot Chips 20, 2008.

[18] M.J.Quinn, "Designing Efficient Algorithms for Parallel Computers", McGraw-Hill, 1987, page 125.

[19] F. Black and M. Scholes, "The pricing of options and corporate liabilities," Journal of Political Economy, 81 (1973), pp. 637–654, 1973.

[20] A. Cassidy and A. Andreou, "Beyond Amdahl Law - An objective function that links performance gains to delay and energy", IEEE Transactions on Computers, vol. 61, no. 8, pp. 1110-1126, Aug 2012.

[21] T. Morad, Weiser U, Kolodny A, Valero M., Ayguade E., "Performance, power efficiency and scalability of asymmetric cluster chip multiprocessors", Computer Architecture Letters, Jan.-June 2006, Volume 5, Issue 1, pages 14 – 17.

[22] A. Hartstein, V. Srinivasan, T. Puzak, and P. Emma, "On the nature of cache miss behavior: is it square root of 2?", Journal of Instruction-Level Parallelism, 2008

[23] Z. Guz, O. Itzhak, I. Keidar, A. Kolodny, A. Mendelson, U. Weiser, "Threads vs. Caches: modeling the behavior of parallel workloads", 2010 IEEE International Conference on Computer Design (ICCD), Oct. 2010, Pages: 274-281.

[24] K. Pagiamtzis and A. Sheikholeslami, "Content-addressable memory (CAM) circuits and architectures: a tutorial and survey," IEEE Journal of Solid-State Circuits, vol. 41, no. 3, pp. 712 – 727, March 2006